Cellulose (2017) 24:951–965
DOI 10.1007/s10570-016-1141-5

ORIGINAL PAPER

Prevention of mold invasion by eco-friendly lignin/polycaprolactone nanofiber membranes for amelioration of public hygiene

Seongpil An · Joo Hyun Hong · Kyo Yong Song · Min Wook Lee · Salem S. Al-Deyab · Jae Jin Kim · Alexander L. Yarin · Sam S. Yoon

Received: 4 August 2016 / Accepted: 18 November 2016 / Published online: 25 November 2016

Abstract Herein, we fabricated highly porous and stretchable electrospun nanofiber membranes using eco-friendly lignin and polycaprolactone polymers, which efficiently prevent mold colonization and invasion in pine sapwood. Membranes of different thicknesses were tested against four species of mold. Membrane thicknesses of above 38 μm were found to completely prevent mold invasion during the 2- and 4-week cultivation periods. The membranes were characterized using various qualitative and quantitative analytical methods, including tensile tests. The optimized fabrication conditions were established to protect wood from mold growth and to accommodate the periodic expansion and contraction of wood without degradation. The mechanically strong and elastic nanofiber membranes enable an assessment of the membrane's suitability and feasibility as an alternative to the existing wallpapers or paints.

Keywords Electrospinning · Lignin · Eco-friendly nanofibers · Mold-related indoor hygiene · Sick-building syndrome

Introduction

Wood has been among the materials most valuable to humans since the beginning of humankind. It is used throughout human life, for example, as a fuel, raw industrial resource, and construction material (Zabel and Morrell 2012). Because wood is easy to handle and renewable with moderate strength and good durability, it has been used for thousands of years in

Seongpil An and Joo-Hyun Hong have contributed equally to this work.

Electronic supplementary material The online version of this article (doi:10.1007/s10570-016-1141-5) contains supplementary material, which is available to authorized users.

S. An · K. Y. Song · A. L. Yarin (✉) · S. S. Yoon (✉)
School of Mechanical Engineering, Korea University, Seoul 02841, Republic of Korea
e-mail: ayarin@uic.edu

S. S. Yoon
e-mail: skyoon@korea.ac.kr

J. H. Hong · J. J. Kim
Division of Environmental Science and Ecological Engineering, Korea University, Seoul 02841, Republic of Korea

M. W. Lee · A. L. Yarin
Department of Mechanical and Industrial Engineering, University of Illinois at Chicago, Chicago, IL 60607-7022, USA

S. S. Al-Deyab
Petrochemical Research Chair, Chemistry Department, King Saud University, Riyadh 11451, Saudi Arabia

construction. However, the use of wood as a building material has been challenged recently because various illnesses have been attributed to exposure to indoor fungi-contaminated environments (Bernstein et al. 2008; Edmondson et al. 2005). This problem is called sick-building syndrome (SBS) or toxic-mold syndrome (TMS), and has become increasingly prevalent since the 1970s (Pettigrew et al. 2010; Redlich et al. 1997). Fungi grow in a broad range of pH and temperature values when the moisture content of wood exceeds 20% (Stienen et al. 2014). Growth is accelerated when the relative humidity exceeds 95% (Viitanen and Ritschkoff 1991). Numerous studies associating fungi and adverse human health effects have been performed (Bush et al. 2006; Clark et al. 2004; Portnoy et al. 2005); however, the issue remains unsolved.

Fungi causing surface discoloration with visible multicellular hyphae are generally called molds. In addition to mottling the surface of materials, molds also produce spores and mycotoxins (or fungal toxins); these mycotoxins negatively affect the human immune system (Heseltine and Rosan 2013; Pettigrew et al. 2010). Symptoms and conditions such as coughing, sneezing, eye irritation, skin rashes, vomiting, asthma, and pneumonitis can be caused by fungi colonizing the body through contact or inhalation (Kiffer and Morelet 1999; Samson et al. 2004; Singh et al. 2010). In sites such as retirement homes, day-care centers, and hospitals, fungi can be fatal. While ventilation and sufficient drying of indoor wood is necessary because of the ubiquity of molds, advanced prevention of mold growth on indoor wood should take precedence over all other measures, because wood supplies nutrition to the molds.

To protect wood from molds outdoors, rapid drying or poisonous chemical treatments are commonly used for the affordability and efficiency of these techniques. However, the toxicity of the chemicals and other problems related to the environment and human health remain as serious concerns (Hong et al. 2014). In addition, some molds are resistant to the toxic chemicals. Antifungal paint is often used for indoor wood; however, cracks inevitably form because of the periodic expansion and contraction of the wood, thus enabling mold growth. For these reasons, a non-toxic environmentally friendly method should be developed to protect wood from molds. A new approach to prevent mold from physically accessing wood is required. Biocompatible soy protein-based electrospun nanofiber membranes were recently revealed to prevent the invasion of grapevines by esca fungi (Sett et al. 2015). To physically block fungi penetration, thus protecting pruning cuts and wounds in the vines from esca fungi, electrospun nanofibers deposited onto mechanically robust rayon membranes were developed (Sett et al. 2015).

Here, porous and stretchable lignin/polycaprolactone (PCL) and PCL-only nanofiber membranes (LPNM and PNM) were fabricated to protect wood against mold invasion. The nanofibers were fabricated by an electrospinning technique which is known as one of the most attractive methods for producing large-size non-woven or woven nanofiber fabrics (An et al. 2016; Persano et al. 2013). In addition, the nanofiber fabrics, where the diameter of nanofibers ranges from tens to hundreds of nm, have a superior surface-to-volume ratio compared to the general fabrics, which facilitates much larger fabric-size produced from a small amount of raw materials without compromising the anti-fungi-barrier features. Lignin is the second-most abundant natural polymeric material, after cellulose, and comprises approximately 20% of annual terrestrial biomass production (Jennings and Lysek 1999; Schmidt 2006). Until recently, lignin was considered a waste byproduct of the pulp and paper industries. However, active study of the material began (Hu and Hsieh 2013; Jennings and Lysek 1999; Nelson et al. 2012; Wahba et al. 2015) after it was recognized as an inexpensive, non-toxic, and eco-friendly carbon-based material. PCL is another biodegradable, non-toxic, and inexpensive polymer that has been used extensively in engineering (Hogan Jr and Niklas 2004; Zhang et al. 2009).

In the present work, we firstly demonstrate a nanometer-scale manufacturing approach for the amelioration of SBS by a mold invasion test. The test was conducted on pine sapwood coated with porous and stretchable membranes of various thicknesses, which elucidated the preventive effect of the membranes against mold invasion. The membranes exhibited excellent prevention capability and mechanical properties by impeding mold invasion velocity to 0.10–0.11 μm/h and yielding only at the high strain value of 82–106%, respectively (in the present context strain means relative elongation).

Materials and methods

Materials for electrospinning solutions

Low-sulfonate alkali lignin (lignin, $M_w = 10$ kDa), polycaprolactone (PCL, $M_n = 80$ kDa), and polyacrylonitrile (PAN, $M_w = 150$ kDa) were used as solutes in the electrospinning solutions. Formic acid (≥95%), acetic acid (99.7%), and dimethylformamide (DMF, 99.8%) were used as solvents. All materials were purchased from Sigma-Aldrich.

Fabrication of lignin/PCL and PCL nanofiber membranes

Solutions of 15 wt% lignin/PCL (lignin-to-PCL ratio of 1:1 w/w) and 15 wt% PCL were prepared by mixing the solutes with a blended solvent of 1:3 w/w formic and acetic acids. For example, 100 g of 15 wt% lignin/PCL solution was prepared from 7.5 g of lignin, 7.5 g of PCL, 21.25 g of formic acid, and 63.75 g of acetic acid. Also, 100 g of 15 wt% PCL solution was prepared from 15 g of PCL, 21.25 g of formic acid, and 63.75 g of acetic acid. The solutions were stirred at 55 °C for 15 h until they became homogenous. To fabricate a large-area thick membrane, as shown in Fig. 1a, the electrospun nanofibers were deposited on a drum collector using a setup with two syringe pumps (Legato 100, KD Scientific) and two DC power supplies (EL20P2, Glassman High Voltage, Inc.). The rotation speed of the drum collector was 200 rpm. Each syringe was equipped with an 18-gauge needle (Nordson EFD) at the exit. The distance between the collector and needles was 6 cm. Note that the electrically-driven polymer jets are issued from the Taylor-cone at the nozzle exit and undergo dramatic thinning process due to the electrically-driven bending instability accompanied by the solvent evaporation. As a result, ultra-thin nanofibers are formed (Reneker and Yarin 2008). The lignin/PCL nanofibers were electrospun at a flow rate of $Q = 200$ μL/h and a high DC voltage of $V = 9$–10 kV. PCL nanofibers were electrospun at $Q = 150$ μL/h and 7–8 kV. After electrospinning was completed, the nanofiber membranes were easily detached from the drum collector.

Mold species and cultivation conditions

Four species of mold were selected for the present tests. *Aspergillus versicolor* KUC5201, *Cladosporium cladosporioides* KUC1385, *Penicillium brevicompactum* KUC1819, and *Trichoderma viride* KUC5062 were obtained from the Korea University Culture collection. The target molds were cultivated on 20 mL of 2% malt extract agar (MEA, Difco) at 25 °C for 2 weeks for sporulation. The inhibition of mold spore germination was tested according to the ASTM standard test method D4445. The size of each specimen was 7 mm by 20 mm in cross-section and 70 mm long and the moisture contents in each specimen was at least 40%. Each unseasoned pine sapwood (*Pinus densiflora*) specimen was covered with the fabricated membranes detached from the drum collector (Fig. 1a). Subsequently, a suspension of the mixed spores was inoculated by spraying onto the specimens, which was adjusted to deliver 400 μL suspension/spray as shown in Fig. 1b. Then, the membrane-wrapped specimens exposed to molds were evaluated after 2 weeks of cultivation.

Tensile test procedure

The stress–strain curves of the membranes were measured in tensile tests using an Instron 5942 machine equipped with a 100 N capacity load cell. The membranes were cut in the machine direction MD into 15 mm × 60 mm pieces and clamped by two pneumatic grips. The initial spacing between the upper and lower grips was fixed to 20 mm, and the strain rate was set to 10 mm/min. The membranes were stretched until complete failure. Tensile tests were repeated ten times per membrane.

Characterization

The morphology and thickness of the membranes were studied by a field-emission scanning electron microscope (FE-SEM, S-5000, Hitachi). The size distribution of the nanofibers was estimated by measuring ~100 nanofibers from the SEM images. Three-dimensional (3D) images were obtained using an optical profiler (Wyko NT1100, Veeco). Brunauer–Emmett–Teller (BET) tests for surface area were conducted in N_2 after 96 h pre-treatment at 50 °C. The crystallinity of the PCL was identified by X-ray diffraction (XRD, SmartLab, Rigaku). Thermogravimetric analysis (TGA, SDT Q600, TA Instruments) and derivative thermogravimetric analysis (DTG) were performed in air at a fixed flow rate of 100 mL/

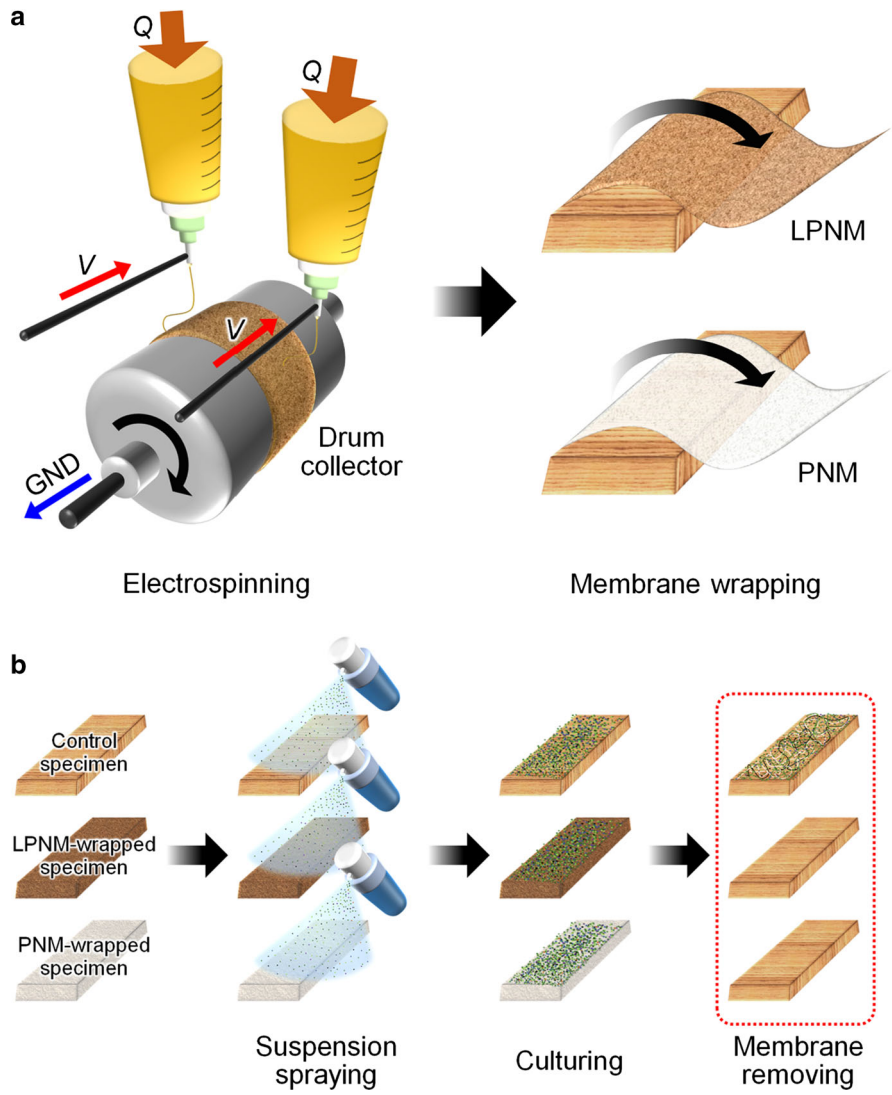

Fig. 1 **a** Schematics of the electrospinning setup and the membrane wrapping. **b** Schematic of the mold invasion test

min and a heating rate of 5 °C/min, using 1–2 mg of membrane material heated from 20 to 600 °C. The mold spores on the surfaces of the specimens and membranes were observed by an optical microscope (SZ61, Olympus) and FE-SEM.

Results and discussion

Lignin/PCL and PCL nanofiber membranes (LPNM and PNM)

The LPNM and PNM were fabricated by electrospinning the precursor solutions for different times to create nanofibrous membranes of different thicknesses. The solvent of the precursor was evaporated during electrospinning, and thus, solidified polymer nanofibers were obtained. Accordingly, the weight ratio of lignin-to-PCL in the LPNM is 1:1. The bulk densities of lignin and PCL are 0.37 and 1.15 g/mL, respectively. Using these values, we estimated the volume ratio of lignin-to-PCL in the LPNM as 3.1:1. Figure 2 shows SEM images of the LPNM and the PNM membranes created using different deposition times (t_{dep}). Uniformly dense LPNM formed at different deposition times are seen in Fig. 2a, whereas the PNM membranes in Fig. 2b reveal the presence of a few thick fibers on the micrometer scale. These

thicker microfibers formed thicker membranes of PNM (35, 42, and 75 µm, respectively) than the ones obtained using LPNM (8, 21, and 38 µm, respectively). The corresponding fiber-size distributions are shown in Supplementary Fig. S1.

To compare the average roughnesses (R_a) and porosities of the membranes, the optical profiler and Brunauer–Emmett–Teller (BET) analyses were used on the $t_{dep} = 9$ h samples, as shown in Figs. 3 and 4a. The LPNM sample had a much lower value of $R_a = 467$ nm (Fig. 3a) than the PNM of $R_a = 828$ nm (Fig. 3b); this is associated with the presence of the micrometer-size PNM fibers mentioned above. In addition, the LPNM sample revealed a surface area four times larger than that of the PNM sample (Fig. 4a), which relates to the corresponding average fiber-diameter difference between the materials in Supplementary Fig. S1. While the above analyses

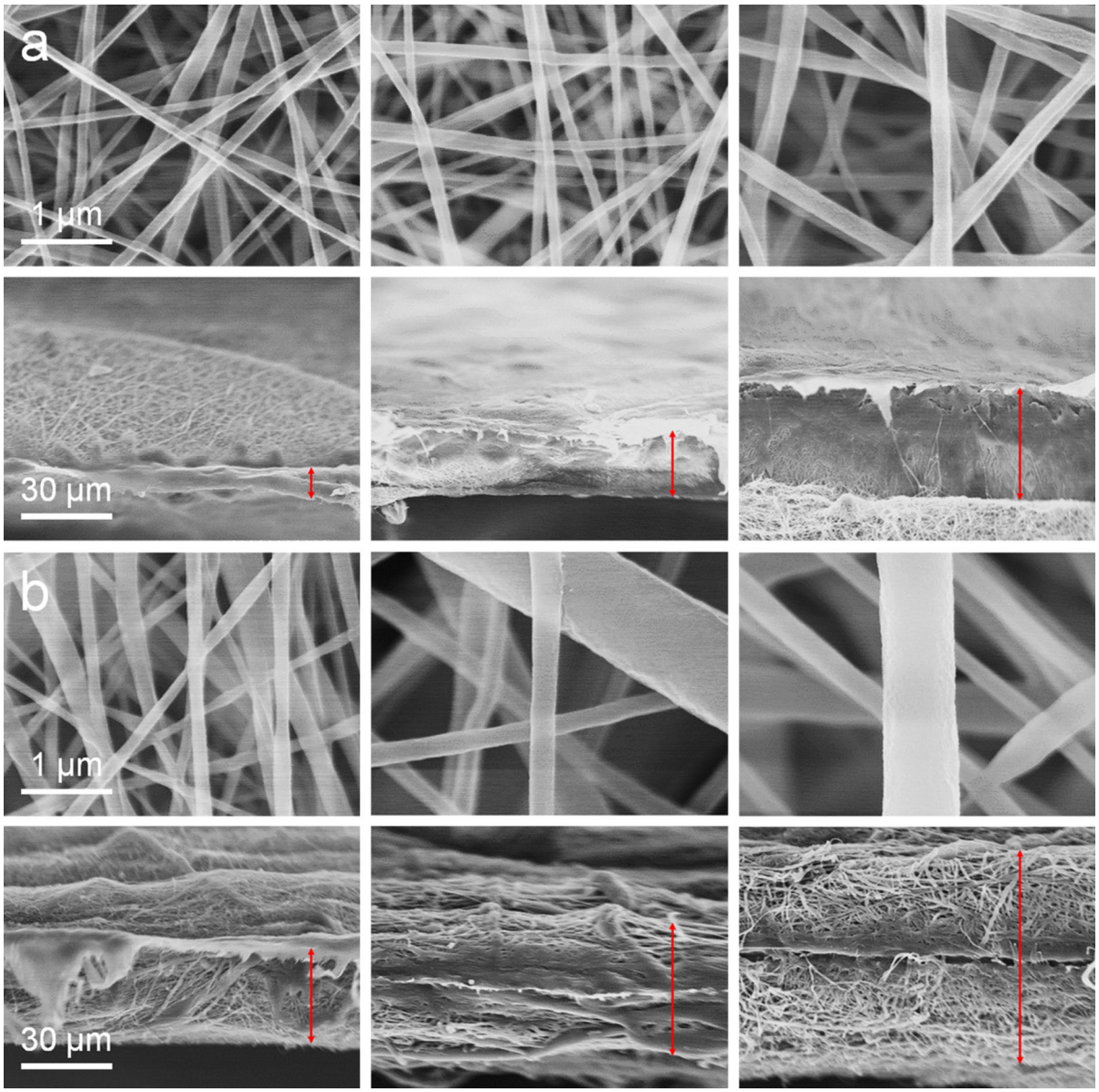

Fig. 2 Top and cross-sectional SEM images of **a** the LPNM and **b** the PNM electrospun at different deposition times. The *first*, *second*, and *third columns* correspond to $t_{dep} = 3$, 6, and 9 h cases, respectively

showed clear distinctions between the LPNM and PNM samples, both samples have similar average pore sizes (Fig. 4a).

Figure 4b shows the XRD patterns of the LPNM and PNM for $t_{dep} = 9$ h. Two high-intensity peaks at $2\theta = 21.5°$ and 23.8°, indicating the presence of PCL, are clearly seen, but the broad peak at $2\theta = 22.5°$ characteristic of amorphous lignin is covered by the PCL peak and thus not exposed (Nelson et al. 2012; Wahba et al. 2015).

The presence of lignin in the LPNM was confirmed by TGA and DTG analyses, as shown in Fig. 4c, d. Major weight loss is observed in both membranes from 100 to 400 °C (Fig. 4c), associated with the decomposition of the organic polymers. To better characterize the thermal decomposition of the LPNM, the DTG curve was obtained (Fig. 4d). The DTG curve clearly shows two peaks at 355 and 423 °C, corresponding to the oxidation of lignin phenolic structures to quinone methides and the decomposition of the quinone methides, respectively (Hu and Hsieh 2013). In the PNM, the peak corresponding to PCL decomposition is located at 387 °C (Zhang et al. 2009).

Prior to the mold invasion test, water solubility testing was conducted as shown in Supplementary Fig. S2. Each membrane was fully wetted and stored at room temperature ($T = 25$ °C) until it had dried completely dried. The solubility of the nanofibers in contact with water was necessary information, both because the mold spore suspension is water-based and because the tested specimens had high moisture contents for culturing the molds. The lignin/PCL nanofibers were only slightly dissolved because of the alkalinity of the lignin, while the PCL nanofibers had not dissolved at all. Despite the slight degradation of LPNM in water, the porous structure was maintained.

Mold invasion test on the control pine sapwood

As stated, *Aspergillus versicola* KUC5201, *Cladosporium cladosporioides* KUC1385, *Penicillium brevicompactum* KUC1819, and *Trichoderma viride* KUC5062 were examined in the invasion test (cf. Fig. 5). Many molds produce mycotoxins, which interfere with RNA synthesis and cause DNA damage. In the case of *A. versicolor*, macrocyclic trichothecenes, trichodermin, and satratoxin G have been reported as mycotoxins. Multiple cases have been documented in which high concentrations of *C. cladosporioides* and *Penicillium chrysogenum* spores caused hypersensitivity pneumonitis (Chiba et al. 2009; Pomés et al. 2016).

The presence of grown mold spores was confirmed by optical microscope and SEM images, as shown in Fig. 6. Broadly filled green-colored spore groups on the surface of the control specimen of pine sapwood are seen in Fig. 6a. Among the four molds used, *T. viride* reveals more significant growth than the other molds, implying antagonism between molds. The genus *Trichoderma* is well known for producing antifungal compounds, secretions of chitinase, and mycoparasites against other fungi and being fast growing. Accordingly, the antagonistic tendency of *T. viride* disrupted the growth of the other molds. For this reason, the genus *Trichoderma* is the most frequently isolated mold found in lumber yards (Schmidt 2006).

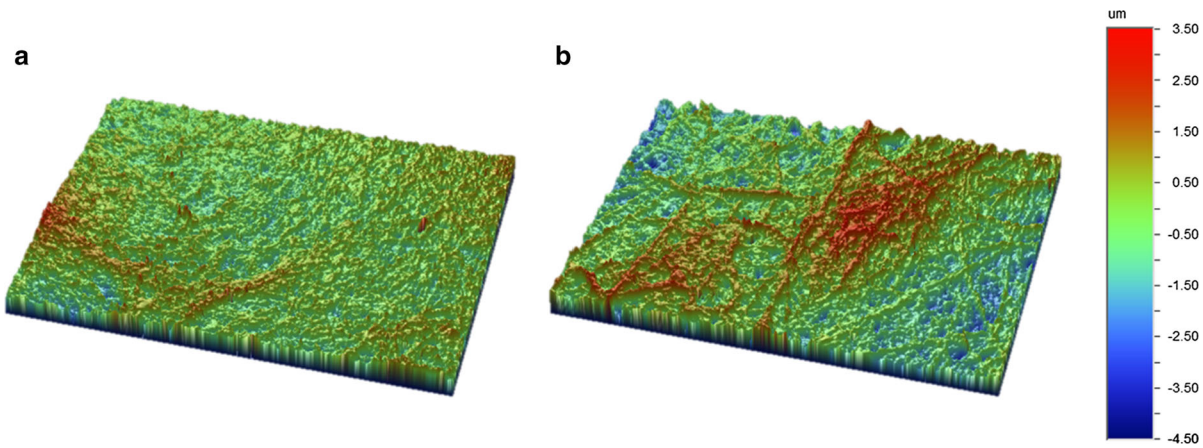

Fig. 3 3D optical profiler images of **a** the LPNM and **b** the PNM

a

	LPNM	PNM
BET specific surface area (m^2/g)	16.54	4.82
Total pore volume (cm^3/g)	0.169	0.120
Average pore size (nm)	40.7	44.1

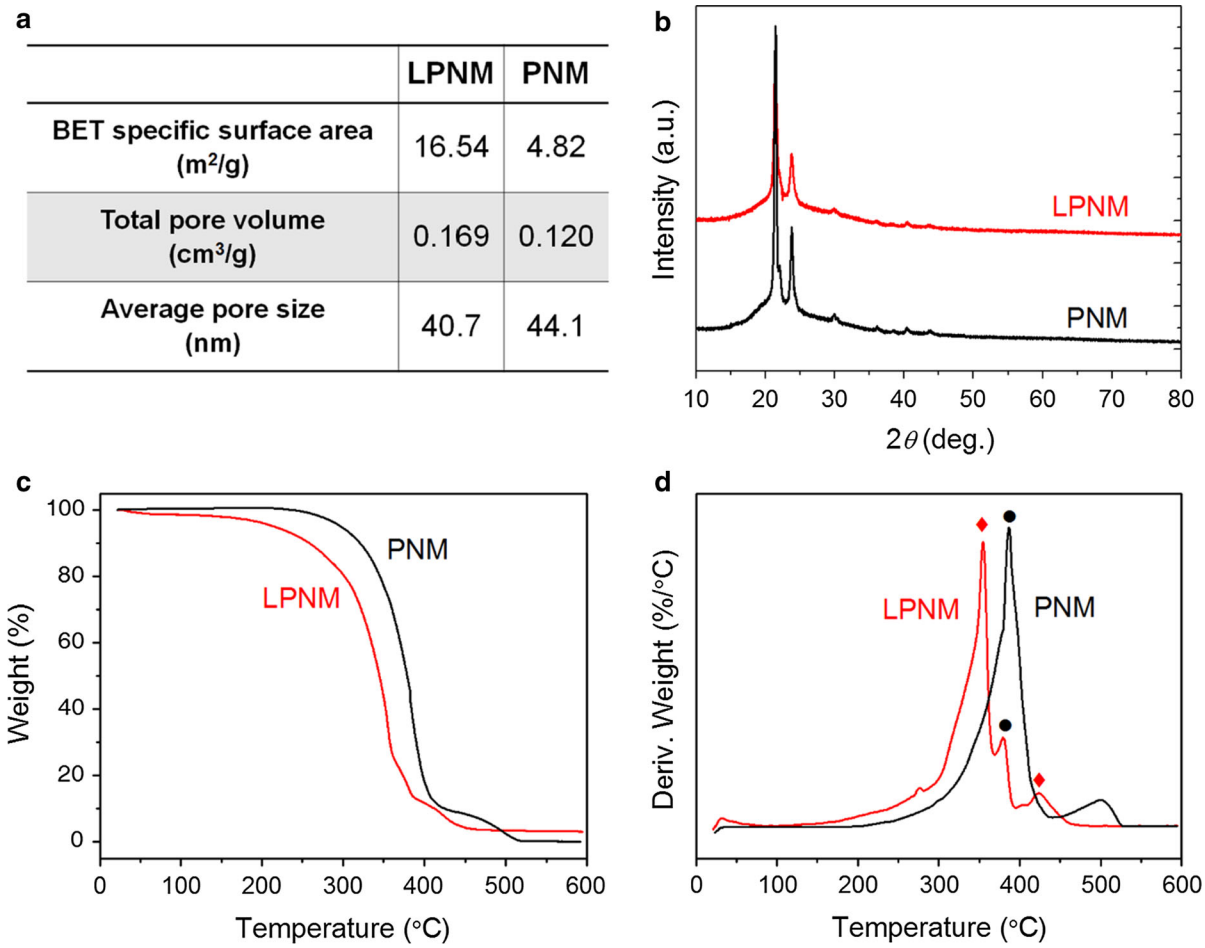

Fig. 4 **a** BET analyses of the membranes. **b** XRD patterns of the membrane. **c** TGA and **d** DTG analyses of the two types of membranes (*filled diamonds* lignin, and *filled circles* PCL)

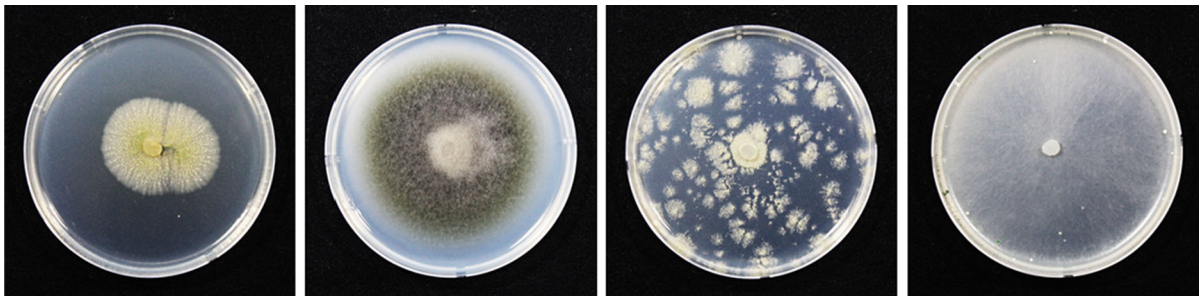

Fig. 5 Photographs of the four molds tested, which correspond to *Aspergillus versicola* KUC5201, *Cladosporium cladosporioides* KUC1385, *Penicillium brevicompactum* KUC1819, and *Trichoderma viride* KUC5062, respectively

Mold invasion test on the LPNM-wrapped pine sapwood

The prevention effect of the membranes against mold invasion of the sapwood was studied, as shown in Figs. 7, 8 and 9. Prior to the invasion test, membranes of various thicknesses were prepared to verify the effect of thickness on mold invasion (cf. Fig. 2). Figure 7 shows the results of the invasion test for the LPNM-wrapped specimens. In contrast with the

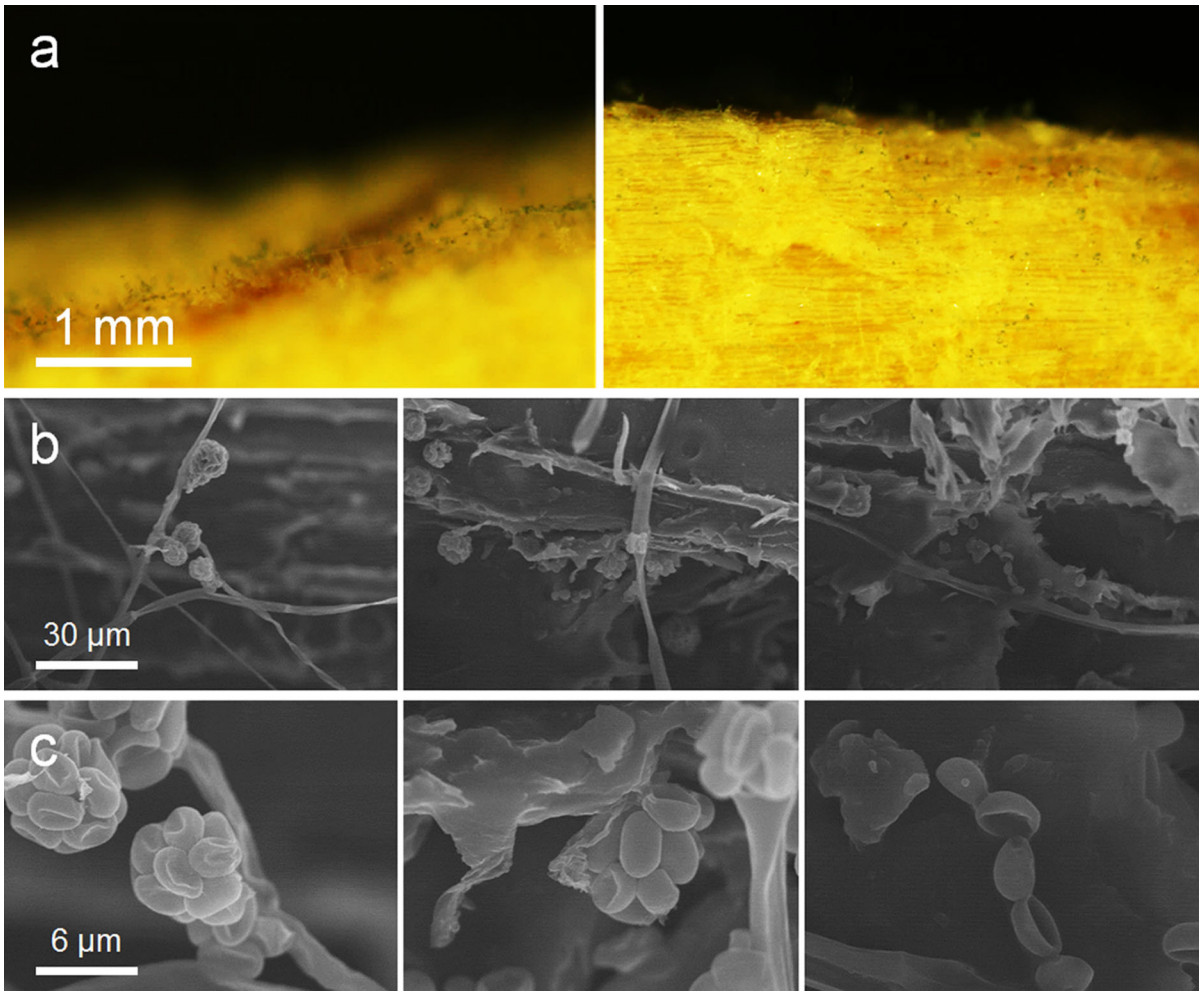

Fig. 6 **a** Optical microscope and **b**, **c** SEM images of the control pine sapwood specimen (without any membrane) after 2 weeks of mold cultivation

control, a slight stain on the top surface of the LPNM-wrapped specimen was observed by eye (Fig. 7b). Interestingly, in the optical microscope images, only a few spores are observed in $t_{dep} = 9$ h case, whereas multiple spores were observed in the $t_{dep} = 3$ and 6 h cases. In order to better characterize and quantify the mold spore growth as the deposition time t_{dep} and, thus, the membrane thickness was increased, the spore-covered areas were evaluated from ten randomly selected SEM images of the tested LPNMs. On $t_{dep} = 3$, 6, and 9 h cases, the covered areas measured 36,710, 26,915, and 15,185 µm^2, respectively, within total studied areas of 114,576 µm^2 each. The growth is reduced with increased t_{dep}. This also implies that the rate of nutrient supply from the wrapped sapwood to the spores depends on the wrapping membrane thickness, diminishing as the thickness increases. This inverse dependence of the nutrition supply on the membrane thickness determines the prevention efficiency, as established in the invasion test and described in the following sections. Note that the above explanation is quite plausible given the moisture content of the specimens of 40%.

Fig. 7 Photographs of the LPNM-wrapped specimens **a** at the beginning and **b** after 2 weeks of mold cultivation. **c** Optical image and **d**, **e** SEM images of the surface of the tested LPNM. The *first*, *second*, and *third columns* correspond to $t_{dep} = 3$, 6, and 9 h cases, respectively

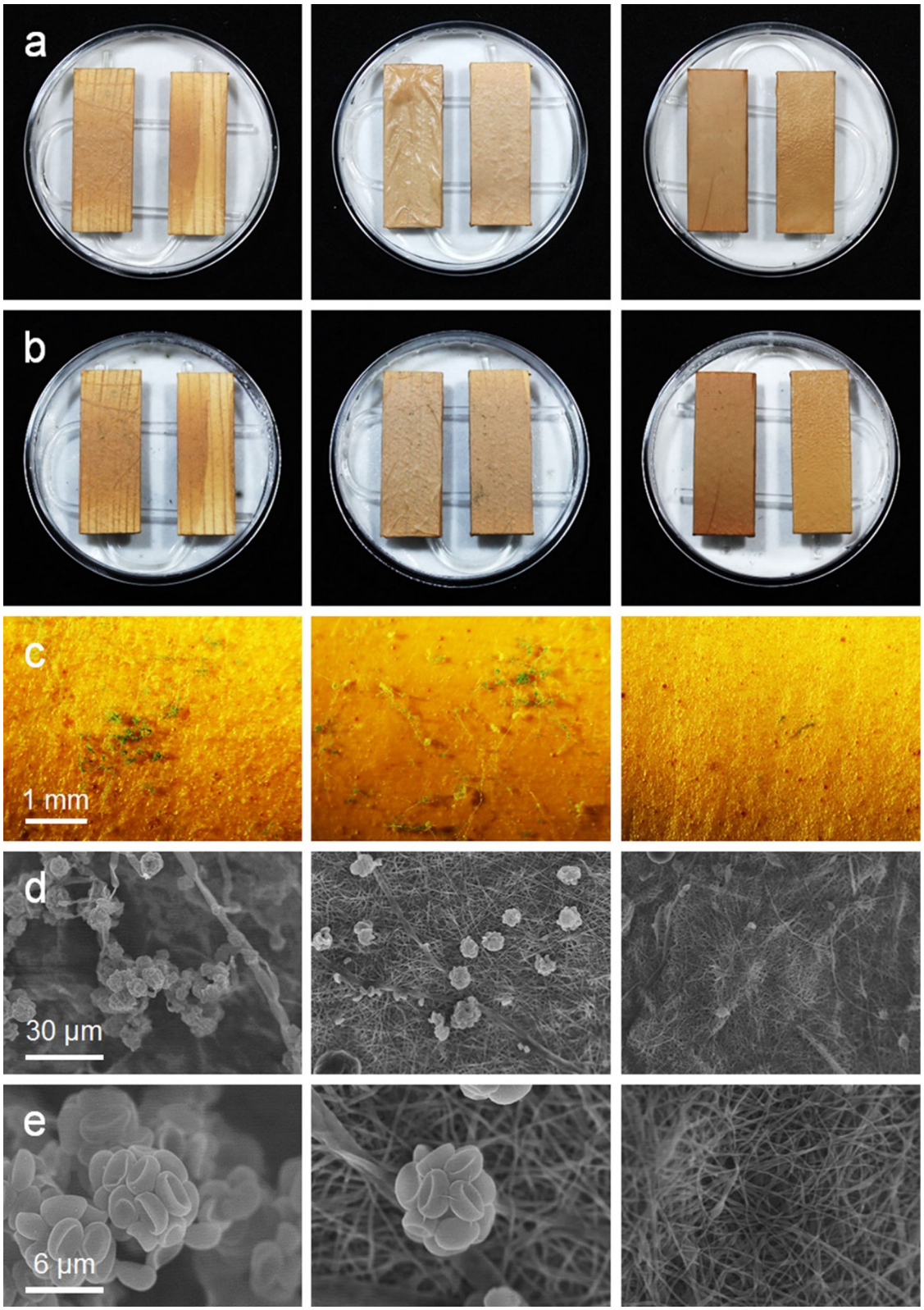
a
b
c
1 mm
d
30 µm
e
6 µm

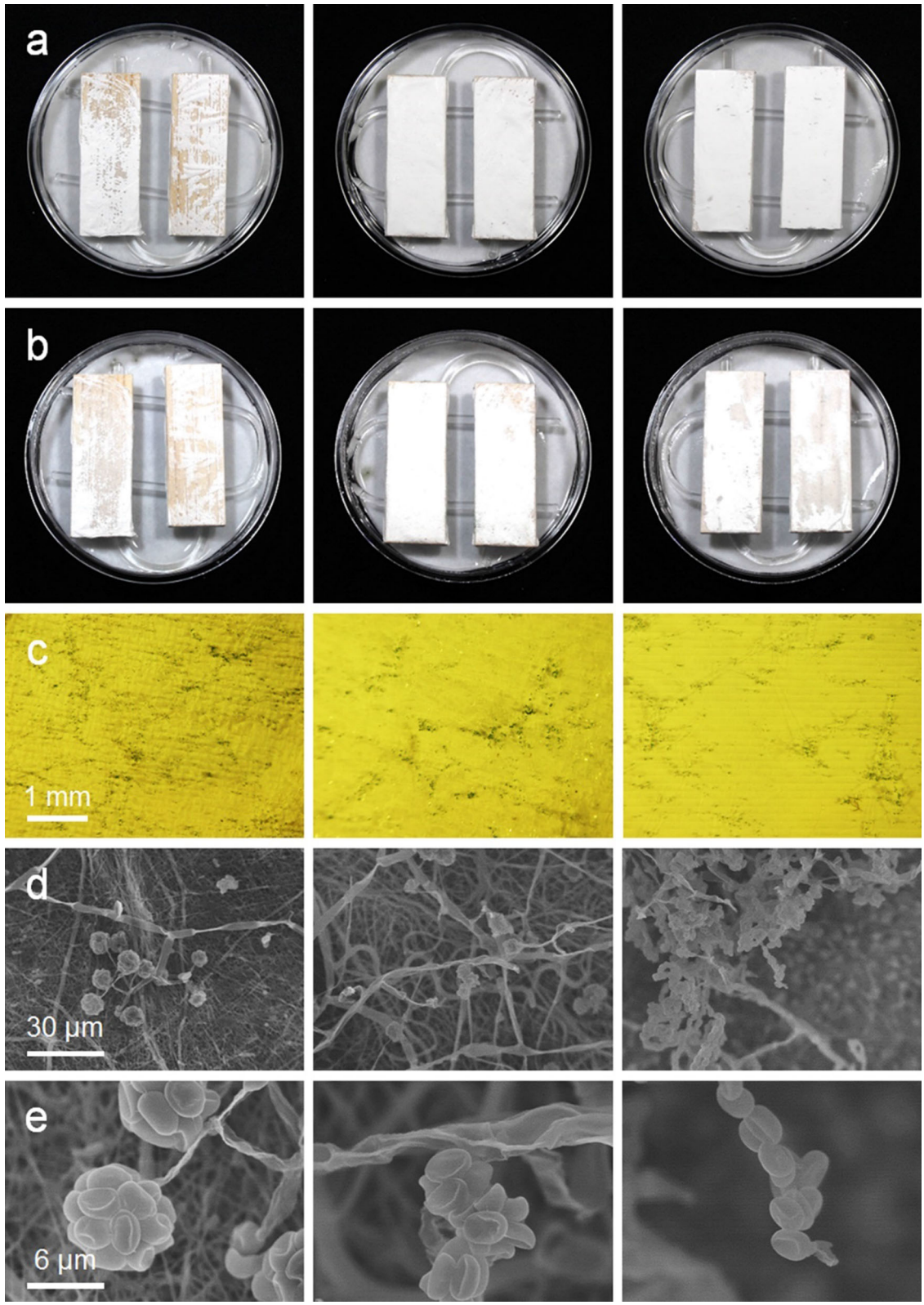
a
b
c
1 mm
d
30 µm
e
6 µm

◀**Fig. 8** Photographs of the PNM-wrapped specimens **a** at the beginning and **b** after 2 weeks of mold cultivation. **c** Optical image, and **d**, **e** SEM images of the surface of the tested PNM. The *first*, *second*, and *third columns* correspond to $t_{dep} = 3$, 6, and 9 h cases, respectively

Mold invasion test on the PNM-wrapped pine sapwood

Figure 8 shows the results of the mold invasion test on the PNM-wrapped specimens. While the size of the agglomerated spores is smaller than that seen in the LPNM case, the overall covered area is larger than that in the LPNM case (cf. Figs. 7c, 8c). The spore-covered areas on the $t_{dep} = 3$, 6, and 9 h cases were 36,604, 20,936, and 15,385 μm^2, respectively, over the same areal size studied in the LPNM case. This also reflects the inverse dependence of the nutrition supply on the membrane thickness, as with LPNM.

Prevention efficiency

The prevention effect of the membrane wrapping as a function of membrane thickness was studied using images from optical microscopy (Fig. 9a–d) and SEM (not shown here) of the tested specimens after membrane removal. The prevention efficiency plotted in Fig. 9d is defined as $\eta = (1 - A/A_0) \times 100\%$, where A is the spore-covered area and A_0 is the total studied area of 233,532 μm^2 in the ten randomly selected SEM images. Most of the specimen surfaces were protected. In the $t_{dep} = 6$ h case of the PNM and $t_{dep} = 9$ h cases of both the LPNM and the PNM, in particular, $\eta = 100\%$ was achieved (Fig. 9). It seems that perfect prevention can be achieved for membrane thicknesses of 35 μm or more during the 2-week cultivation period; $\eta = 99\%$ for $t_{dep} = 3$ h case of the PNM (cf. Figs. 2, 9). The mold invasion velocity, optimized under our experimental conditions, is defined as $V_{invasion} = D/t$. Here, D is the mold invasion distance and t is the cultivation time. The invasion distance in this study was set to 35 μm $< D <$ 38 μm because η of 99% and 100% were achieved in the $t_{dep} = 3$ h case of the PNM and the $t_{dep} = 9$ h case of the LPNM (which had the smallest thickness among all $\eta = 100\%$ cases), respectively. The cultivation time was 336 h, exactly 2 weeks. Accordingly, $V_{invasion}$ is evaluated as 0.10–0.11 μm/h. While this velocity could change for different kinds of fibers, fungi, and experimental conditions, the membrane thickness can be controlled selectively for the target cultivation time.

We conducted an additional mold invasion test using the LPNM-wrapped specimens during a 4-week cultivation period as shown in Fig. S4. At the deposition times $t_{dep} = 3$ and 6 h, the mold invasions were clearly observed by the optical microscope images (Figs. S4a and S4b), which was a natural consequence based on the estimated value of the invasion velocity $V_{invasion}$. However, it should be emphasized that a complete prevention of fungi invasion was repeatedly achieved at $t_{dep} = 9$ h even during the 4-week cultivation period. Based on the $V_{invasion}$ value of 0.10–0.11 μm/h, in the case of $t_{dep} = 9$ h corresponding to the 38 μm thickness (cf. Fig. 2a), the coating should have been penetrated after 772 h (4 weeks) by the molds. Thus, we anticipate that there could be a threshold value of the membrane thickness to prevent mold invasion permanently.

Prevention mechanism

Before confirming the prevention mechanism of the membranes, the growth of molds on biodegradable versus non-biodegradable membranes were studied, because it was possible that molds could obtain nutrients by consuming the biodegradable components of lignin or PCL, regardless of the nutrition supply from the sapwood. A solution of 8 wt% PAN in DMF was used to fabricate non-biodegradable membranes at $Q = 200$ μL/h and $V = 6.5$ kV. Supplementary Fig. S3 shows the results of the 2-week cultivation in the absence of wood under the same cultivation conditions. In all cases, no spore growth is observed, verifying that the tested molds cannot consume either lignin or PCL. Accordingly, it seems that the molds sprayed onto the wrapped specimens had survived by consuming nutrition from the sapwood, which was decomposed by the cellulolytic enzymes from the molds and transported through the membrane pores, as illustrated in Fig. 10. Furthermore, the molds generated very thin fiber-shaped hypha (cf. Figs. 7, 8), which could penetrate pores of 40–44 nm in size as well as tens of micrometers through the membranes (Fig. 4a), thus enabling mold invasion. As a result, spores were formed on the surfaces of the wrapped specimens (Fig. 10b).

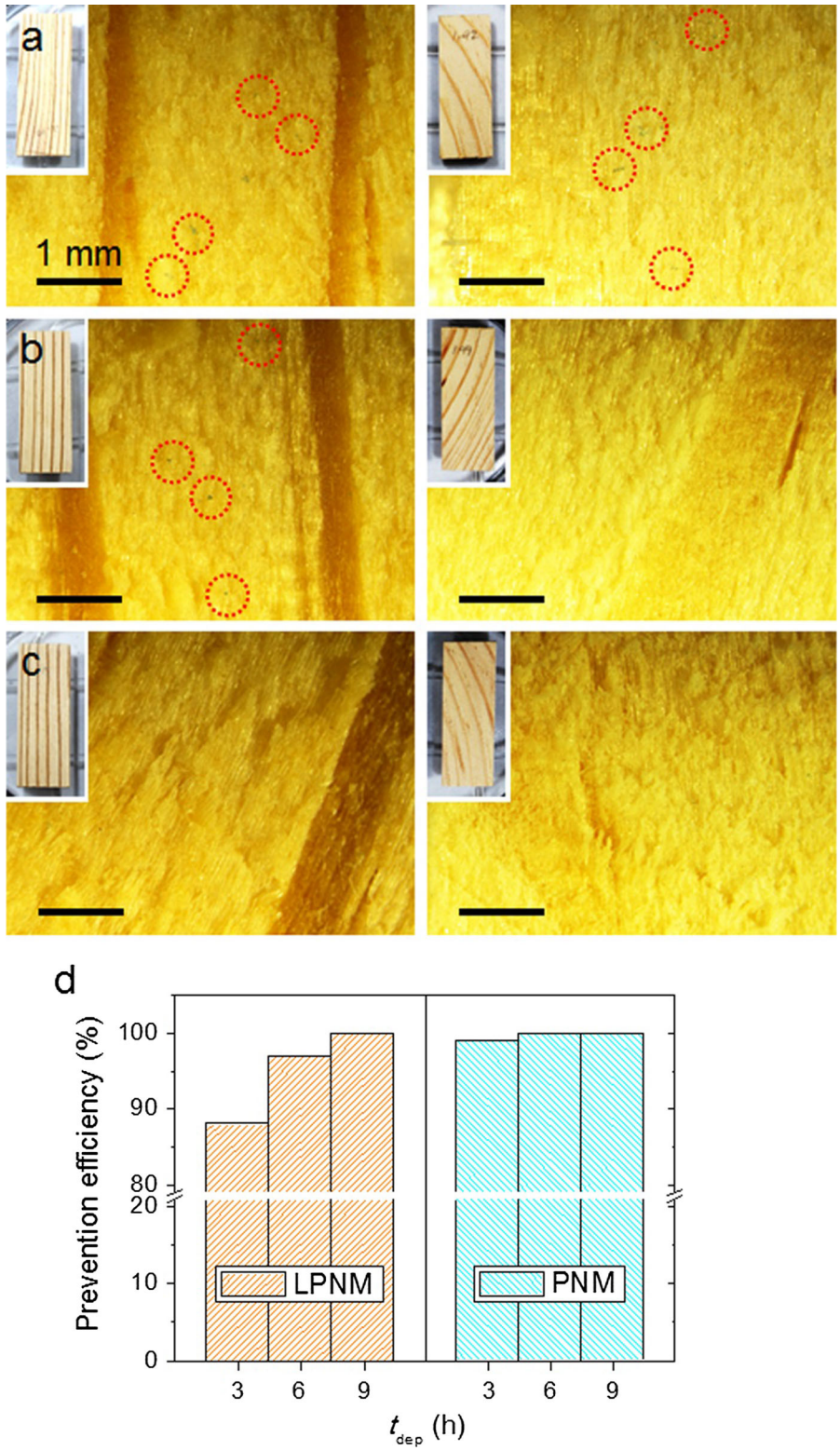

Fig. 9 (*Left column*) Photographs and optical microscope images of the specimens after the LPNM had been removed, and (*right column*) the specimens after the PNM had been removed after 2 weeks of mold cultivation. The **a** *first*, **b** *second*, and **c** *third rows* correspond to $t_{dep} = 3$, 6, and 9 h cases, respectively. **d** Prevention efficiency of the membranes against mold invasion

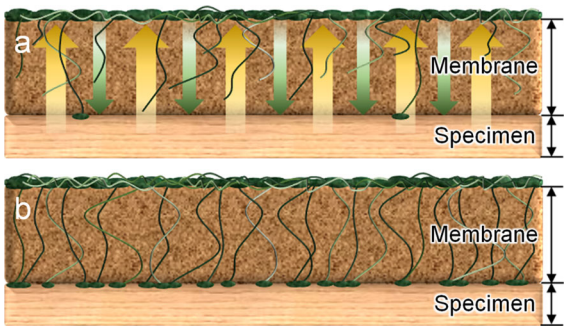

Fig. 10 Prevention mechanism of the membranes. **a** During mold cultivation. *Green* and *yellow arrows* represent cellulolytic enzyme and nutrition moving paths, respectively. **b** After 2 weeks of mold cultivation. (Color figure online)

Results of tensile tests

It is important to measure the mechanical properties of the membranes because wood experiences periodic expansion and contraction following the surrounding environmental conditions (such as changes in temperature and humidity) (Hogan Jr and Niklas 2004). While manufactured lumber and specimens thereof do not change in dimensions as significantly as living wood does, they still periodically expand and contract.

Stress–strain curves measured at 10 mm/min for LPNM and PNM are shown in Fig. 11a, b, respectively. In Fig. 11c, the phenomenological elasto-plastic model Green equation:

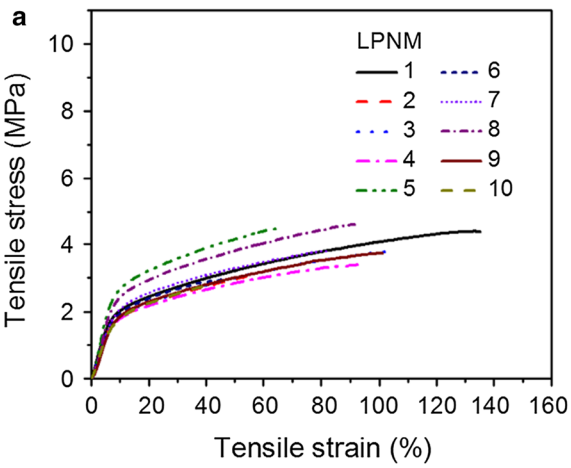

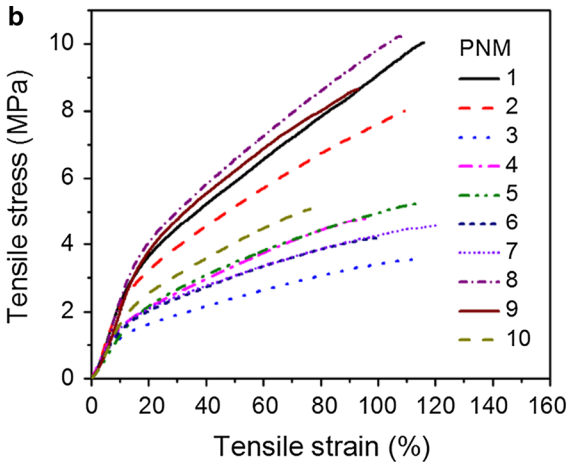

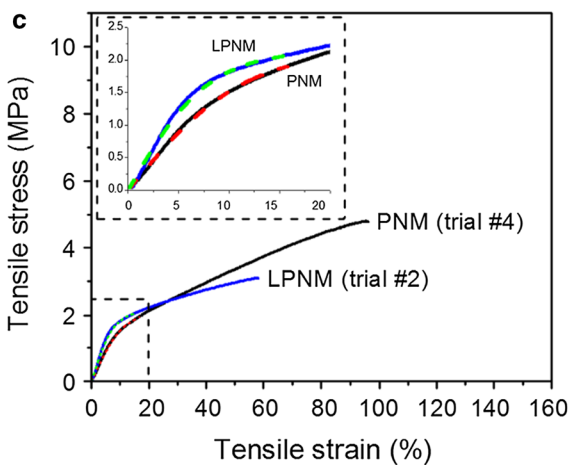

d

	LPNM	PNM
E (MPa)	25.95 ± 6.60	16.94 ± 3.36
σ_{max} (MPa)	3.69 ± 0.64	6.43 ± 2.53
ε_f (%)	81.94 ± 29.17	105.51 ± 13.37

Fig. 11 Stress-strain curves of **a** the LPNMs and **b** the PNMs. **c** An example of fitting the Green equation (the *green* and *red dashed line* for the LPNM and PNM, respectively). **d** Average values of Young's modulus, ultimate stress, and strain-at-failure, respectively. (Color figure online)

$$\sigma_{xx} = Y \tanh\left(\frac{E}{Y}\varepsilon_{xx}\right) \quad (1)$$

was fitted to the experimental data; σ_{xx} is the tensile stress, E is the Young's modulus, Y is the yield stress, and ε_{xx} is the tensile strain.

The measured stress and strain values at failure (σ_{max} and ε_f, respectively), as well as the Young's modulus and yield stress (E and Y, respectively), are summarized in Supplementary Tables S1 and S2. As discussed previously (Lee et al. 2015), the Green equation encompasses the entire elastic response of a membrane, including the transition into perfect plasticity. In the membranes used in this study, the transition into perfect plasticity did not occur completely. For this reason, the fitting range was bounded at the beginning of the early plastic region, after the elastic part in the curve. In some cases, the fitting accuracy was $\sim$99%. The blended nanofiber membranes (PNM) had lower ultimate strength and strain-at-failure values compared to LPNM. According to Sett et al. (2015), soy protein/nylon 6 nanofiber mats have less resistance to stretching than pure nylon 6 nanofiber mats do. Similarly, in the present case, blending PCL with lignin lowers the strain-at-failure and the ultimate strength of the PNM.

Conclusions

Enhanced indoor hygiene can be attained by using both eco-friendly lignin/PCL and PCL nanofiber membranes. These naturally-obtained lignin-based membranes are more eco-friendly and economic compared to the existing wallpapers or anti-fungal paints because lignin is obtained from waste byproducts, whereas the existing wallpapers or paints are produced using petroleum-derived materials. In addition, the membrane replacement time for preventing a further spore spread can be estimated in advance by the invasion velocity. Thus, the membranes developed in the present work hold great promise as an alternative to the existing wallpapers or paints. Large-area membranes of different thicknesses were prepared by electrospinning polymers or polymer blends onto a drum collector. To demonstrate the prevention effect of the membranes, mold invasion tests were conducted on control and membrane-wrapped pine sapwood specimens using a mixed suspension of four species of mold spores. Complete prevention of mold invasion was achieved for membranes of either material with thicknesses of 35 μm or greater. The membrane thickness can be selectively optimized according to the mold invasion velocity calculated in the present study. The highly porous structure of the membrane hinders both the paths of the cellulolytic enzymes from the molds and the nutrition supply from the wood, while providing breathability for the wood, which ultimately physically blocks the spread of mold in an eco-friendly way. In addition, tensile tests revealed the elasticity and durability of the membranes, illustrating their capability to survive periodic expansions and contractions of wood.

Acknowledgments This work was primarily supported by the Industrial Strategic Technology Development Program (Grant 10045221) funded by the Ministry of Knowledge Economy (MKE, Korea). This work was also supported by the Global Frontier Hybrid Interface Materials (GFHIM) of NRF-2013M3A6B1078879, NRF-2012-Fostering Core Leaders of the Future Basic Science Program of NRF-2012H1A8003235 and the Commercializations Promotion Agency for R&D Outcomes (COMPA) funded by the Ministry of Science, ICT and Future Planning (MISP). S.S.Y. expresses his thanks to the support made by King Saud University, Vice Deanship of Research Chairs.

References

An S, Lee MW, Jo HS, Al-Deyab SS, Yoon SS (2016) Weaving nanofibers by altering counter-electrode electrostatic signals. J Aerosol Sci 95:67–72

Bernstein JA et al (2008) The health effects of nonindustrial indoor air pollution. J Allergy Clin Immunol 121:585–591

Bush RK, Portnoy JM, Saxon A, Terr AI, Wood RA (2006) The medical effects of mold exposure. J Allergy Clin Immunol 117:326–333

Chiba S et al (2009) Cladosporium species-related hypersensitivity pneumonitis in household environments. Intern Med 48:363–367

Clark N et al (2004) Damp indoor spaces and health. National Academies Press, Washington

Edmondson DA, Nordness ME, Zacharisen MC, Kurup VP, Fink JN (2005) Allergy and "toxic mold syndrome". Ann Allergy Asthma Immunol 94:234–239

Heseltine E, Rosan J (2013) WHO guidelines for indoor air quality: dampness and mould, vol 92. WHO Regional Office for Europe, Copenhagen

Hogan CJ Jr, Niklas KJ (2004) Temperature and water content effects on the viscoelastic behavior of *Tilia americana* (Tiliaceae) sapwood. Trees 18:339–345

Hong JH, Lee J, Min M, Ryu SM, Lee D, Kim GH, Kim JJ (2014) 6-Pentyl-α-pyrone as an anti-sapstain compound produced by *Trichoderma gamsii* KUC1747 inhibits the

germination of ophiostomatoid fungi. Holzforschung 68:769–774
Hu S, Hsieh Y-L (2013) Ultrafine microporous and mesoporous activated carbon fibers from alkali lignin. J Mater Chem A 1:11279–11288
Jennings DH, Lysek G (1999) Fungal biology: understanding the fungal lifestyle. Bios Scientific Publishers, Oxford
Kiffer E, Morelet M (1999) The deuteromycetes. Mitosporic fungi: classification and generic keys. Science Publishers, Enfield
Lee MW et al (2015) Polyacrylonitrile nanofibers with added zeolitic imidazolate frameworks (ZIF-7) to enhance mechanical and thermal stability. J Appl Phys 118:245307
Nelson MT, Munj HR, Tomasko DL, Lannutti JJ (2012) Carbon dioxide infusion of composite electrospun fibers for tissue engineering. J Supercrit Fluids 70:90–99
Persano L, Camposeo A, Tekmen C, Pisignano D (2013) Industrial upscaling of electrospinning and applications of polymer nanofibers: a review. Macromol Mater Eng 298(5):504–520
Pettigrew HD, Selmi CF, Teuber SS, Gershwin ME (2010) Mold and human health: separating the wheat from the chaff. Clin Rev Allergy Immunol 38:148–155
Pomés A, Chapman MD, Wünschmann S (2016) Indoor allergens and allergic respiratory disease. Curr Allergy Asthma Rep 16:1–10
Portnoy JM, Kwak K, Dowling P, VanOsdol T, Barnes C (2005) Health effects of indoor fungi. Ann Allergy Asthma Immunol 94:313–320
Redlich CA, Sparer J, Cullen MR (1997) Sick-building syndrome. Lancet 349:1013–1016
Reneker DH, Yarin AL (2008) Electrospinning jets and polymer nanofibers. Polymer 49:2387–2425
Samson RA, Hoekstra ES, Frisvad JC (2004) Introduction to food-and airborne fungi, vol 7. Centraalbureau voor Schimmelcultures (CBS), Utrecht
Schmidt O (2006) Wood and tree fungi. Springer, Heidelberg
Sett S, Lee MW, Weith M, Pourdeyhimi B, Yarin A (2015) Biodegradable and biocompatible soy protein/polymer/adhesive sticky nano-textured interfacial membranes for prevention of esca fungi invasion into pruning cuts and wounds of vines. J Mater Chem B 3:2147–2162
Singh J, Yu CWF, Kim JT (2010) Building pathology, investigation of sick buildings—toxic moulds. Indoor Built Environ 19:40–47
Stienen T, Schmidt O, Huckfeldt T (2014) Wood decay by indoor basidiomycetes at different moisture and temperature. Holzforschung 68:9–15
Viitanen H, Ritschkoff A (1991) Mould growth in pine and spruce sapwood in relation to air humidity and temperature. Swedish University of Agricultural Sciences, Uppsala
Wahba SM, Darwish AS, Shehata IH, Elhalem SSA (2015) Sugarcane bagasse lignin, and silica gel and magneto-silica as drug vehicles for development of innocuous methotrexate drug against rheumatoid arthritis disease in albino rats. Mater Sci Eng C 48:599–610
Zabel RA, Morrell JJ (2012) Wood microbiology: decay and its prevention. Academic Press, Syracuse
Zhang J, Xu J, Wang H, Jin W, Li J (2009) Synthesis of multiblock thermoplastic elastomers based on biodegradable poly (lactic acid) and polycaprolactone. Mater Sci Eng C 29:889–893